

Unravelling the Nature of a Toluene-Fumaronitrile Complex

SUPPLEMENTARY MATERIALS

Andrzej J. Kałka, Mateusz Z. Brela, Andrzej M. Turek*

Faculty of Chemistry, Jagiellonian University,
30-387 Kraków, Gronostajowa 2, Poland

*Corresponding Author
turek@chemia.uj.edu.pl

Co-authors e-mail addresses:
andrzej.kaalka@doctoral.uj.edu.pl, mateusz.brela@uj.edu.pl

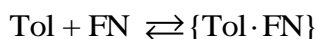
List of contents:

1. Extended theoretical background	
1.1 Thermodynamic complex stability constant	2
(Formulas: S.1, S.2, S.3)	
1.2 Enthalpy and entropy of complex formation	5
(Formulas: S.4, S.5a,b)	
2. Technical aspects and methodological details	
2.1 Basis set	6
2.2 Theoretical predictions of the thermodynamical parameters	6
(Formulas: S.6, S.7, S.8a,b)	
2.3 Reproduction and 'idealization' of the measured spectra	8
(Figure Fig. S.1)	
2.4 Selective elimination of toluene spectral contribution, criterion of 'smoothness'	9
(Figure Fig. S.2)	
2.5 Inner filter correction of fluorescence spectra	10
(Formulas: S.9, S.10)	
3. Obtained results	
3.1 Adduct spatial structure and geometry	11
(Tables: Tab. S.1, Tab. S.2; Figures: Fig. S.3, Fig. S.4a,b)	
3.2 Infrared spectra	15
(Tables Tab. S.3; Figures: Fig. S.5a,b, Fig. S.6)	
3.3 Characteristics of vertical electronic excitations	17
(Tables: Tab. S.4, Tab. S.5, Tab. S.5, Tab. S.6)	
(Figures: Fig. S.7, Fig. S.8)	
3.4 Thermodynamic parameters	20
(Tables: Tab. S.7, Tab. S.8, Tab. S.9)	
3.5 Fluorescence in the system	22
(Figures: Fig. S.9, Fig. S.10)	
4. References	23

1. Extended theoretical background

1.1 Thermodynamic complex stability constant

On the basis of the assumption that the investigated complex is characterized by 1:1 stoichiometry, the equilibrium



in the toluene (Tol) - fumaronitrile (FN) system would be described as:

$$K = \frac{[\text{CT}]}{[\text{Tol}] \cdot [\text{FN}]} = \frac{[\text{CT}]}{(\text{Tol}_0 - [\text{CT}]) \cdot (\text{FN}_0 - [\text{CT}])}$$

where K – equilibrium constant, $[\text{CT}]$, $[\text{Tol}]$ and $[\text{FN}]$ – concentrations of complex, free toluene and fumaronitrile at equilibrium, Tol_0 , FN_0 – initial (total) concentrations of toluene and fumaronitrile.

Upon solving the above quadratic equation with respect to $[\text{CT}]$ variable, the formula describing the dependence of the concentration of the formed complex on the initial concentrations of both constituents is obtained [1 - 3]:

$$[\text{CT}] = \frac{\text{FN}_0 \cdot K + \text{Tol}_0 \cdot K + 1 \pm \sqrt{\Delta}}{2K} \quad (\text{S.1})$$

$$\Delta = \text{FN}_0^2 \cdot K^2 - 2\text{FN}_0 \cdot \text{Tol}_0 \cdot K^2 + 2\text{FN}_0 \cdot K + \text{Tol}_0^2 \cdot K^2 + 2 \cdot \text{Tol}_0 \cdot K + 1$$

The above fairly intricate equation can be simplified by suitably designed experiments. By using a significant excess of one of the components (here it is toluene) the original equilibrium equation can be written to a good approximation as [4 - 5]:

$$K = \frac{[\text{CT}]}{\text{Tol}_0 \cdot (\text{FN}_0 - [\text{CT}])}$$

The expression which defines the value of the concentration of the formed adduct as a function of the initial concentrations of Tol_0 and FN_0 is then given by the formula

$$[\text{CT}] = \frac{\text{FN}_0 \cdot K \cdot \text{Tol}_0}{K \cdot \text{Tol}_0 + 1} \quad (\text{S.2})$$

By relating the concentration of the complex to the absorbance A_{CT} of the CT band, it is possible to

calculate its formation constant K and molar absorption coefficient ε_{CT} with the use of the Lambert-Beer law, provided the optical path length, l , is known.

$$A_{CT} = \varepsilon_{CT} \cdot l \cdot [CT]$$

It is accomplished by a fit of the curves given by equations (S.1) and (S.2) to the data obtained from absorptiometric measurements.

Equation (S.2) can also be linearized to a well-known expression, originally proposed by Benesi and Hildebrand [4 - 5]:

$$\frac{FN_0}{A_{CT}} = \frac{1}{K \cdot \varepsilon_{CT} \cdot l} \cdot \frac{1}{Tol_0} + \frac{1}{\varepsilon_{CT} \cdot l}$$

The sought parameters K and ε_{CT} are then directly related to the slope and offset of the fitted straight line.

For the alternative method of equilibrium constant determination (3) based on comparing the mutual signal ratio r (see **Section 2.1**):

$$r = \frac{A_{CT,B}}{A_{CT,A}} = \frac{[CT_B]}{[CT_A]}$$

the use of proper statistical apparatus is required. This is due to the fact that by solving the equation (5):

$$\frac{[CT_A]}{(FN_{0,A} - [CT_A]) \cdot (Tol_{0,A} - [CT_A])} = \frac{[CT_B]}{(FN_{0,B} - [CT_B]) \cdot (Tol_{0,B} - [CT_B])}$$

written in general form as:

$$\frac{x}{(a-x) \cdot (b-x)} = \frac{r \cdot x}{(c-r \cdot x) \cdot (d-r \cdot x)}$$

the following solution for x is obtained:

$$x = \frac{r \cdot (a + b - c - d) \pm \sqrt{\Delta}}{2 \cdot (r - r^2)} \quad (S.3)$$

$$\Delta = a^2 \cdot r^2 + 4 \cdot a \cdot b \cdot r^3 - 2 \cdot a \cdot b \cdot r^2 - 2 \cdot a \cdot c \cdot r^2 - 2 \cdot a \cdot d \cdot r^2 + b^2 \cdot r^2 - 2 \cdot b \cdot c \cdot r^2 - 2 \cdot b \cdot d \cdot r^2 + c^2 \cdot r^2 - 2 \cdot c \cdot d \cdot r^2 + 4 \cdot c \cdot d \cdot r + d^2 \cdot r^2$$

Thus, for each pair out of the total amount of N samples, one gets a series of independently calculated roots $x = [CT_A]$, and thus a series of the equilibrium constants K . The final outcome should therefore be an average of all such values. Picking up the median or the modal value also seems to be justified. The set of the values of K should then be prevalidated, by neglecting the non-physical solutions or outliers, if they occur. For that purpose, Grubbs statistical test may be successfully used. In the present work, the Authors used Grubbs test implemented in OriginPro 9.1, at the 90% significance level [6].

By the analysis of formulae (S.1) and (S.2), it can be stated, that reliability of the K constant determination depends strongly on the selection of the compared pairs of samples. The stronger the departure from linearity in the signal vs concentration plot is (see for example **Fig. 9**), the more unequivocally determined the equilibrium constant is. This is why the Authors suggest to estimate the final equilibrium constant not by an arithmetic, but a weighted average.

Since the dependence given by (S.1) and (S.2) becomes less linear when: a) the total concentration of the substance in excess (here – toluene) rises and b) difference in concentrations of the compared samples is higher, the Authors used the following 'recipe' for the weights estimation, valid for the applied experiment. Statistic weight w , for the particular 'partial' K to be averaged, is given by:

$$w = (N - n + 1) \cdot (n - m), \quad m < n$$

where N – total amount of the samples in the series (ordered in the monotonically descending order of the toluene concentration ($n = 1$ corresponds to the highest concentration)), n , m – indices of the mutually compared samples, with higher (m) and lower concentration of toluene (n), respectively. Finally, all individual weights are normalized to a unit sum:

$$w' = \frac{w}{\sum_N w}$$

1.2 Enthalpy and entropy of complex formation

By combining the formulae for free enthalpy G and standard free enthalpy G^0 , where H^0 – and S^0 – standard enthalpy and entropy, T – temperature and R – universal molar gas constant

$$\begin{aligned}\Delta G &= \Delta G^0 + RT \cdot \ln K \\ \Delta G^0 &= \Delta H^0 - T \cdot \Delta S^0\end{aligned}$$

for a system in equilibrium ($\Delta G = 0$), a linear relationship between natural logarithm of the equilibrium constant, $K_{(T)}$, and temperature, T , is obtained [7 - 10].

$$\ln K_{(T)} = \frac{-\Delta H^0}{R} \cdot \frac{1}{T} + \frac{\Delta S^0}{R}$$

This formula (4), known as the van't Hoff equation, allows for determining the standard enthalpy ΔH^0 and entropy ΔS^0 of the complex formation, assuming that these values do not change significantly with temperature.

Since the measured systems often do not meet this assumption (see for instance [9]), a deviation from linearity in the van't Hoff plot is not a rare phenomenon. The correction can then be made taking into account the thermal variability of the determined parameters.

The first type of the modification is based on the introduction to formula (4), through Kirchhoff's law, an additional explicit relationship linking the changes of ΔH^0 and ΔS^0 with the standard heat ΔCp^0 of the complex formation [7]:

$$\begin{aligned}\Delta H_{(T)}^0 &= \Delta H_{298K}^0 + \int_{298K}^T \Delta Cp^0 dT = \Delta H_{298K}^0 + \Delta Cp^0 \cdot (T - 298K) \\ \Delta S_{(T)}^0 &= \Delta S_{298K}^0 + \int_{298K}^T \frac{\Delta Cp^0}{T} dT = \Delta S_{298K}^0 + \Delta Cp^0 \cdot \ln (T - 298K)\end{aligned}\tag{S.4}$$

The second common type of the correction consists in expressing the van't Hoff relationship not as a straight line but as a parabola [7 - 8, 10]:

$$\ln K_{(T)} = a + b \cdot \frac{1}{T} + c \cdot \frac{1}{T^2}\tag{S.5a}$$

with empirical coefficients that are related to the sought values of the thermodynamic functions in question [7, 10]:

$$\begin{aligned}\Delta H_{(T)}^0 &= -R \cdot \left(b + 2 \cdot c \cdot \frac{1}{T} \right) \\ \Delta S_{(T)}^0 &= R \cdot \left(a - c \cdot \frac{1}{T^2} \right)\end{aligned}\tag{S.5b}$$

allowing to determine the values of ΔH^0 and ΔS^0 at the standard temperature of 298.15 K.

2. Technical aspects and methodological details

2.1 Basis set

On the basis of the preliminary calculations, 6-311++G** Pople basis set was chosen to be finally applied in the study. The relatively good accuracy with acceptable computational cost was achieved. A set of the diffused functions included in the basis, seems to allow for better description of the long range interactions (noticeable difference between basis set with and without diffused functions implemented).

Counterpoise error, estimated for the chosen basis set, results in overestimation of the absolute value of the complexation energy by less than 10% (c.a. 2 kJ/mol relative to the total complexation energy of ~30 kJ/mol, calculated with CAM-B3LYP in vapour).

2.2 Theoretical predictions of the thermodynamical parameters

Values of the standard enthalpy and entropy of the complex formation were calculated as:

$$\begin{aligned}\Delta H_F &= H_{CT} - (H_{FN} + H_{Tol}) \\ \Delta S_F &= S_{CT} - (S_{FN} + S_{Tol})\end{aligned}$$

where indices CT, FN and Tol refer to molar thermodynamic functions of complex, fumaronitrile and toluene, respectively. The equilibrium constant of complex formation, K_x , was estimated by expression, referring to Boltzman distribution:

$$K_x = \exp \left\{ \frac{-(\Delta H_F - T \cdot \Delta S_F)}{RT} \right\}\tag{S.6}$$

where temperature $T = 298.15$ K, R – universal gas constant.

Values of the 'crude' thermodynamic functions, obtained as described above, were any way recalculated, taking into account two types of corrections.

Type 1) Correction for the unspecific solvent-like interactions of fumaronitrile with toluene, ΔH_{ns} , estimated by PCM approximation of toluene as continuous solvent, was performed as:

$$\begin{aligned}\Delta H_{ns} &= (H_{FN(Tol)} - H_{FN(Vapour)}) \\ \Delta H_{F\ corr} &= \Delta H_F - \Delta H_{ns} \\ \Delta S_{F\ corr} &= \Delta S_F - \frac{\Delta H_{ns}}{T}\end{aligned}\tag{S.7}$$

$\Delta H_{F\ corr}$, and $\Delta S_{F\ corr}$ stands for corrected values of enthalpy and entropy of the adduct formation, respectively. $H_{FN(Vapour)}$, and $H_{FN(Tol)}$ – refer to molar enthalpies of fumaronitrile, calculated in vacuum and in the simulated toluene medium; temperature T is equal to 298.15 K.

Type 2) Adjustment of the mole-fraction-like equilibrium constant, K_X (S.6), connected with its redefinition to the K_C form, based on the molar concentrations $K_C(I)$, (S.1).

$$K_C = K_X \cdot \frac{RTC^\circ}{p} \approx 24.5 \cdot K_X\tag{S.8a}$$

C° , p and T stand for the standard molar concentration (1 M), pressure ($p = 1,013 \cdot 10^5$ Pa), and temperature ($T = 298.15$ K).

Since K_C type of equilibrium constant is used for experimental determination of the complex formation entropy (4),

$$-\frac{\Delta H}{RT} + \frac{\Delta S_C}{R} = \ln K_C = \ln K_X + \ln 24.5 = -\frac{\Delta H}{RT} + \frac{\Delta S_X}{R}$$

the calculated ΔS_X value should also be transformed into ΔS_C , in order to better reflect the experimental conditions.

$$\Delta S_C = \Delta S_X - R \cdot \ln 24.5\tag{S.8b}$$

2.3 Reproduction and 'idealization' of the measured spectra

Toluene-fumaronitrile mixture spectra, recorded in the series, were each time modeled with the use of *Singular Value Decomposition* (SVD) algorithm:

$$\mathbf{X} = \mathbf{USV}^T$$

$$\mathbf{X} \approx \bar{\mathbf{U}}\bar{\mathbf{S}}\bar{\mathbf{V}}^T$$

It means that all matrices \mathbf{X} , containing the total amount of n spectra each, were reproduced as products of the SVD matrices \mathbf{U} , \mathbf{S} and \mathbf{V} , truncated to f principal (significant) factors (two or three, representing toluene, CT band, and residual thermochromic effects), as shown on the example [11]:

$$\mathbf{U} = [\bar{\mathbf{u}}_1, \bar{\mathbf{u}}_2, \dots, \bar{\mathbf{u}}_f, \mathbf{u}_{f+1}, \dots, \mathbf{u}_n]$$

$$\bar{\mathbf{U}} = [\bar{\mathbf{u}}_1, \bar{\mathbf{u}}_2, \dots, \bar{\mathbf{u}}_f]$$

For the thermospectral datasets, the procedure of data 'idealization' was also applied. All the significant vectors \mathbf{v} , collected in the \mathbf{V} matrix (abstract intensity profiles), were replaced with their best possible polynomial (parabolic) fits [12]. Finally, if it was only possible, the 'original' spectra were additionally modeled with a combination of Voigt profiles.

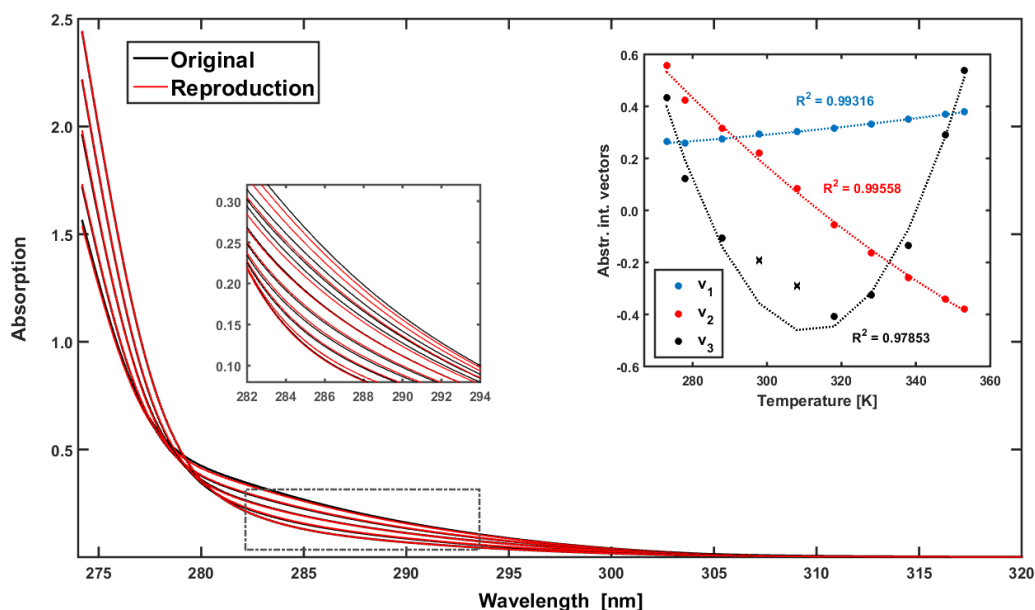


Fig. S.1 Data reproduction procedure, shown on the example of thermally evolving spectra of Tol-FN mixture, recorded in methylcyclohexane. In the main panel, the reproduced spectra (red lines) are compared to the 'crude' ones (black lines). In the right panel, the procedure of eigenvectors 'idealization' by parabolic fit is shown (x – outlier points). For the sake of clarity, only each second spectrum of all acquired is presented in the main window.

2.4 Selective elimination of toluene spectral contribution - criterion of 'smoothness'

As a criterion of successful toluene signal elimination from the spectra of a Tol-FN mixture (see **Fig. 8**), the lack of vibronic bands in the difference spectrum was adopted, since signal representing the remaining CT band(s) is expected to take form of a 'smooth' gaussian-like curve.

The search for the desired difference spectrum was performed iteratively. The spectrum of 'pure' toluene, scaled by a set of discrete values, was each time subtracted from the spectrum of the mixture. The obtained this way difference spectrum was smoothed with a high-grain Whittaker smoother [13] and eventually compared to the original one by *residual sum of squares* (RSS). The difference spectrum, for which a minimum of the RSS is obtained, refers to the optimal one. The whole procedure is schematically depicted below (**Fig. S.2**).

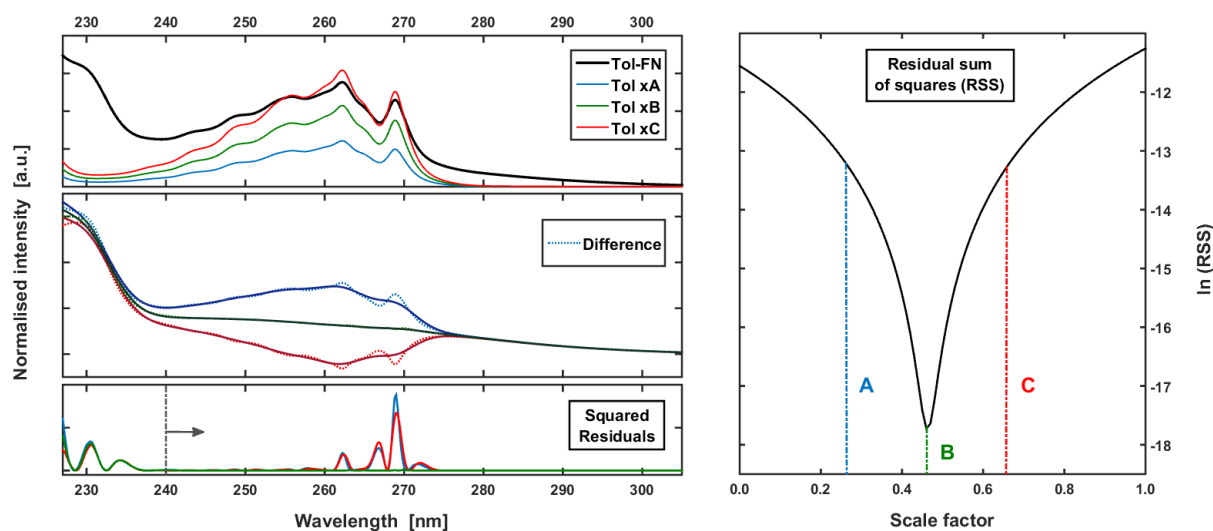


Fig. S.2 Scheme of the algorithm allowing to eliminate a contribution to the mixture spectra from toluene. The spectrum of 'pure' toluene is scaled by a set of discrete values (as example - A, B, C) and subtracted from the spectrum of the mixture (upper panel). Next, for the resulting difference spectrum (middle panel) before and after smoothing, the residuals are calculated (lower panel). Optimal difference spectrum (green) is found, when RSS value reaches its minimum (here – point B).

2.5 Inner filter correction of fluorescence spectra

On the basis of the absorption spectra, recorded for each sample, the fluorescence spectra have been corrected for self absorption, A , of the initially emitted light I_0 (II type of the inner filter effect)[14 - 15],

$$I_{out} = I_0 \cdot 10^{-A} \quad (S.9)$$

by applying the above formula to the measured values of the 'attenuated' fluorescence I_{out} .

Due to the relatively high optical density of the samples ($A > 1$), the recorded signal was also corrected for the 'direct' inner filter effect (I type) [14]. Consequently, the intensity of fluorescence, recorded for all the samples, was standardized (scaled) to the same amount of light absorbed by toluene (reference – solution of 'pure toluene'). The effective 'portion' of toluene-absorbed light, I_{abs} , was estimated for each sample with formula:

$$I_{abs} = \sum_{n=1}^N \Delta I_{abs}(n) = \sum_{n=1}^N I_0 \cdot (10^{-(n-1) \cdot \Delta A_{Sample}}) \cdot (1 - 10^{-\Delta A_{Tol}}) \quad (S.10)$$

which numerically approximates a continuous increase of light absorbed by toluene, ΔI_{abs} , on the optical path, divided into N equally spaced infinitely thin 'layers' of the solution. The formula is based on the well known relationship [14 - 15]:

$$I_{abs} = I_0(n) \cdot (1 - 10^{-A_{Tol}})$$

where $I_0(n)$ denotes intensity of the light falling on the n -th 'layer' of the solution. Since, due to Beer-Lamber law, absorbance is directly proportional to the length of the optical path, 'partial' absorbance, ΔA , is obtained by division of the total absorbance, A , by the total number N of the 'slices':

$$\Delta A_{Sample} = \frac{A_{Sample}}{N} \quad \Delta A_{Tol} = \frac{A_{Tol}}{N}$$

A_{Sample} refers to the total absorbance of the sample (contributions from all substances), while A_{Tol} stands for the absorbance coming only from toluene.

3. Obtained results

3.1 Adduct spatial structure and geometry

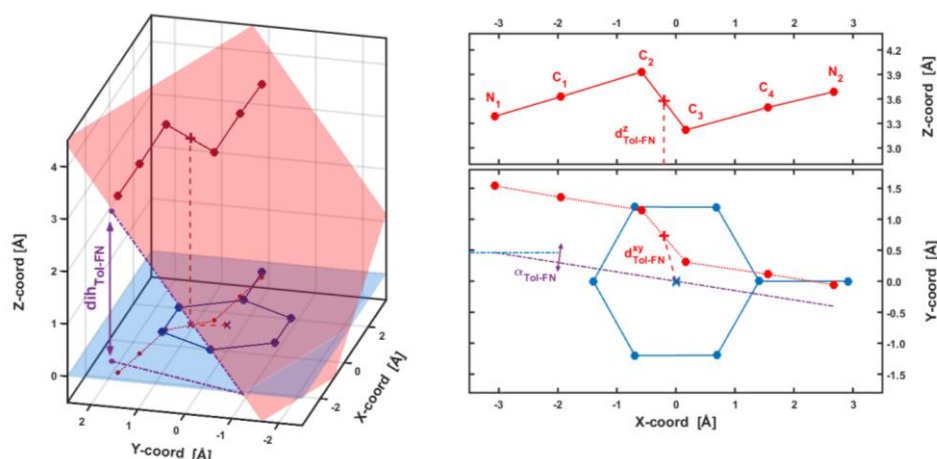


Fig. S.3 Schematic description of the geometrical parameters used in the analysis of Tol-FN adduct spatial structure.

Tab. S.1 Structural parameters of Tol-FN adduct in the ground state, assigned to different solvents.

Solvent:	Vapour $\epsilon = 1.00$	Toluene $\epsilon = 2.37$	THF $\epsilon = 7.43$	n-Pentanol $\epsilon = 15.13$	Ethanol $\epsilon = 24.85$	Acetonitrile $\epsilon = 35.69$
CAM-B3LYP						
dih_{Tol-FN} [deg]	51.36	50.62	49.35	48.87	48.65	48.54
α_{Tol-FN} [deg]	-8.57	-5.65	-4.47	-4.02	-3.83	-3.73
d_{Tol-FN} [Å]	3.655	3.660	3.660	3.660	3.659	3.659
$RMSD_{Tol}$ [Å]	0.007	0.006	0.006	0.006	0.006	0.006
$RMSD_{FN}$ [Å]	0.015	0.010	0.007	0.007	0.007	0.007
B3LYP						
dih_{Tol-FN} [deg]	49.24	49.28	-	46.66	-	47.37
α_{Tol-FN} [deg]	-10.66	-21.19	-	-28.55	-	-20.68
d_{Tol-FN} [Å]	3.637	3.652	-	3.644	-	3.646
$RMSD_{Tol}$ [Å]	0.008	0.006	-	0.005	-	0.007
$RMSD_{FN}$ [Å]	0.018	0.012	-	0.009	-	0.008
M06-2X						
dih_{Tol-FN} [deg]	42.82	42.11	41.32	41.04	40.89	40.64
α_{Tol-FN} [deg]	-4.71	-1.05	-14.79	-14.82	-14.85	-0.89
d_{Tol-FN} [Å]	3.501	3.512	3.520	3.521	3.520	3.516
$RMSD_{Tol}$ [Å]	0.032	0.016	0.033	0.033	0.033	0.018
$RMSD_{FN}$ [Å]	0.128	0.096	0.081	0.076	0.075	0.070
M06-HF						
dih_{Tol-FN} [deg]	35.11	34.94	35.25	34.96	34.82	34.74
α_{Tol-FN} [deg]	-82.23	-82.97	-83.39	-82.28	-82.03	-81.91
d_{Tol-FN} [Å]	3.412	3.418	3.410	3.412	3.412	3.412
$RMSD_{Tol}$ [Å]	0.051	0.055	0.111	0.114	0.114	0.115
$RMSD_{FN}$ [Å]	0.131	0.086	0.059	0.054	0.052	0.051

Tab. S.1 Continuation

Solvent:	Vapour $\epsilon = 1.00$	Toluene $\epsilon = 2.37$	THF $\epsilon = 7.43$	n-Pentanol $\epsilon = 15.13$	Ethanol $\epsilon = 24.85$	Acetonitrile $\epsilon = 35.69$
M06-L						
dih _{Tol-FN} [deg]	44.77	36.70	35.47	35.24	35.23	35.16
α_{Tol-FN} [deg]	-12.84	-58.58	-58.64	-59.10	-59.36	-59.44
d _z [Å]	3.540	3.525	3.527	3.530	3.530	3.531
RMSD _{Tol} [Å]	0.029	0.042	0.060	0.062	0.062	0.063
RMSD _{FN} [Å]	0.114	0.116	0.100	0.097	0.096	0.095
PBE0						
dih _{Tol-FN} [deg]	46.66	51.08	50.12	49.71	49.50	49.39
α_{Tol-FN} [deg]	-28.55	-21.44	-21.32	-20.82	-20.61	-20.51
d _z [Å]	3.644	3.634	3.635	3.636	3.636	3.635
RMSD _{Tol} [Å]	0.005	0.005	0.005	0.005	0.005	0.005
RMSD _{FN} [Å]	0.009	0.011	0.008	0.007	0.007	0.007
MP2						
dih _{Tol-FN} [deg]	47.37	47.23	-	36.94	-	36.64
α_{Tol-FN} [deg]	-14.52	-21.52	-	80.81	-	81.23
d _z [Å]	3.495	3.504	-	3.446	-	3.446
RMSD _{Tol} [Å]	0.016	0.016	-	0.091	-	0.092
RMSD _{FN} [Å]	0.109	0.069	-	0.056	-	0.053
LC-ωPBE						
dih _{Tol-FN} [deg]	43.30	42.70	-	36.92	-	35.61
α_{Tol-FN} [deg]	-37.82	-40.53	-	73.31	-	-65.41
d _z [Å]	3.542	3.552	-	3.504	-	3.507
RMSD _{Tol} [Å]	0.001	0.001	-	0.012	-	0.016
RMSD _{FN} [Å]	0.022	0.0154	-	0.008	-	0.009
LC-BLYP (without GD3)						
dih _{Tol-FN} [deg]	90.01	67.48	-	123.12	-	69.82
α_{Tol-FN} [deg]	0.01	8.52	-	-5.02	-	4.62
d _z [Å]	3.913	3.839	-	3.766	-	3.887
RMSD _{Tol} [Å]	0.003	0.002	-	0.004	-	0.002
RMSD _{FN} [Å]	0.000	0.002	-	0.003	-	0.001

For geometrical parameters see **Fig. S.3**; ϵ_{rel} – relative dielectric constant taken from [16]; RMSD value is related to atomic deviations from molecular plane; for LC-BLYP functional, the Grimme empirical dispersion correction (GD3) was not added, as it is not implemented in Gaussian 16 A.

Since the results obtained with LC-BLYP method significantly differ from all the others, they are not included in the later sections.

Tab. S.2 Structural parameters of Tol-FN adduct in their excited states in vapour.

State	S ₀	S ₁	S ₂	S ₃	S ₄
TDA-CAM-B3LYP					
dih _{Tol-FN} [deg]	51.36	37.55	32.62	46.36	32.13
$\alpha_{\text{Tol-FN}}$ [deg]	-8.57	-6.17	3.16	9.51	3.16
d _z [Å]	3.655	3.407	3.407	3.665	3.407
RMSD _{Tol} [Å]	0.007	0.028	0.004	0.013	0.004
RMSD _{FN} [Å]	0.015	0.258	0.183	0.012	0.182
TDA-M06-2X					
dih _{Tol-FN} [deg]	42.82	28.15	28.14	1.60	59.26
$\alpha_{\text{Tol-FN}}$ [deg]	-4.71	-3.69	-3.70	2.51	-6.73
d _z [Å]	3.501	3.368	3.368	3.131	3.571
RMSD _{Tol} [Å]	0.032	0.054	0.054	0.244	0.117
RMSD _{FN} [Å]	0.128	0.745	0.745	0.031	0.119

For geometrical parameters see **Fig. S.3**;

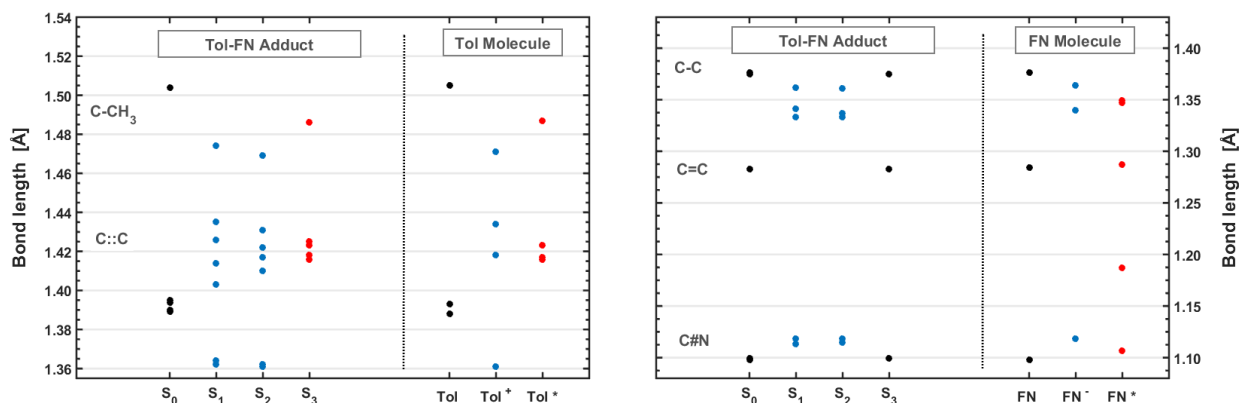


Fig. S.4a Bond lengths within the Tol-FN complex at different (excited) states, compared to their equivalents calculated for the isolated molecules of toluene (left panel) and fumaronitrile (right panel) in their neutral, ionic (radical) and excited forms. Performed ‘match’, suggesting which particular form of the molecule is observed in the different electronic states of the complex, is depicted in black, blue and red. The TDA-CAM-B3LYP method.

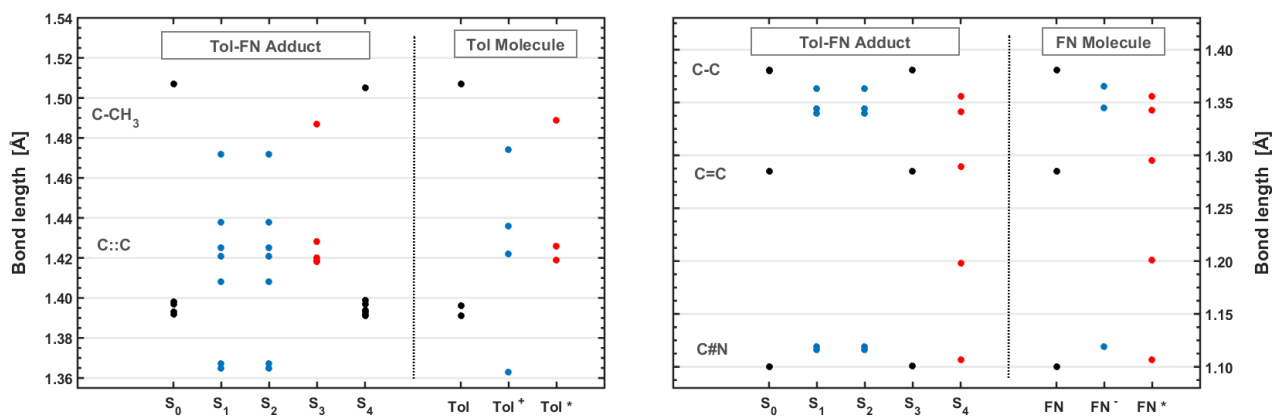


Fig. S.4b Comparison of bond lengths same as in Fig. S.4a, but for the TDA-M06-2X method.

3.2 Infrared spectra

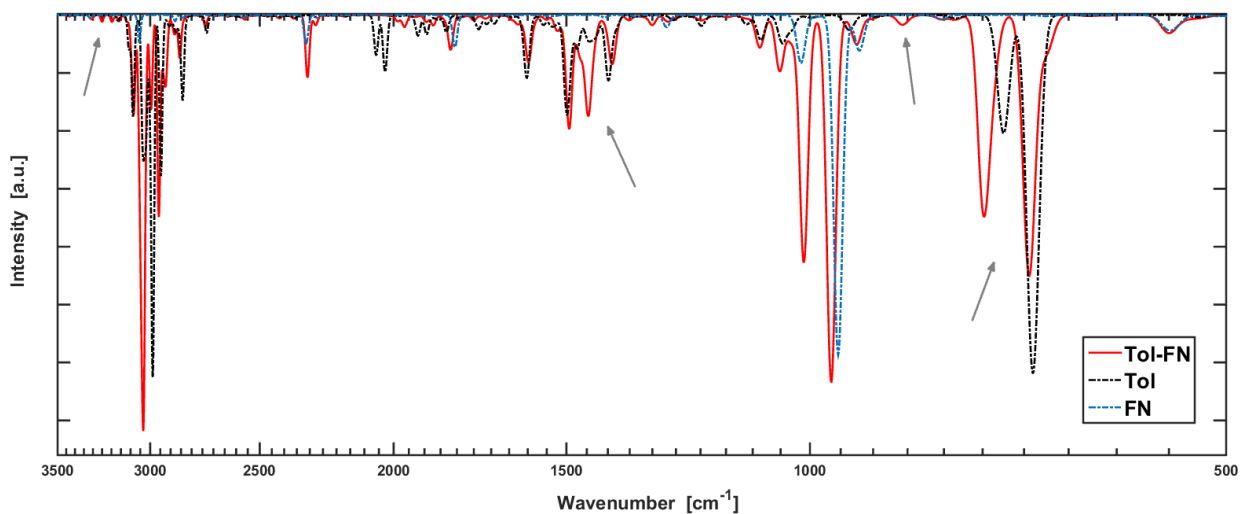


Fig. S.5a Infrared spectra of toluene, fumaronitrile and their adduct simulated in anharmonic approximation (B3LYP). The changes strongly correlated with experiment are indicated with arrows. For other methods see **Fig. 3** and **Fig 5.b**.

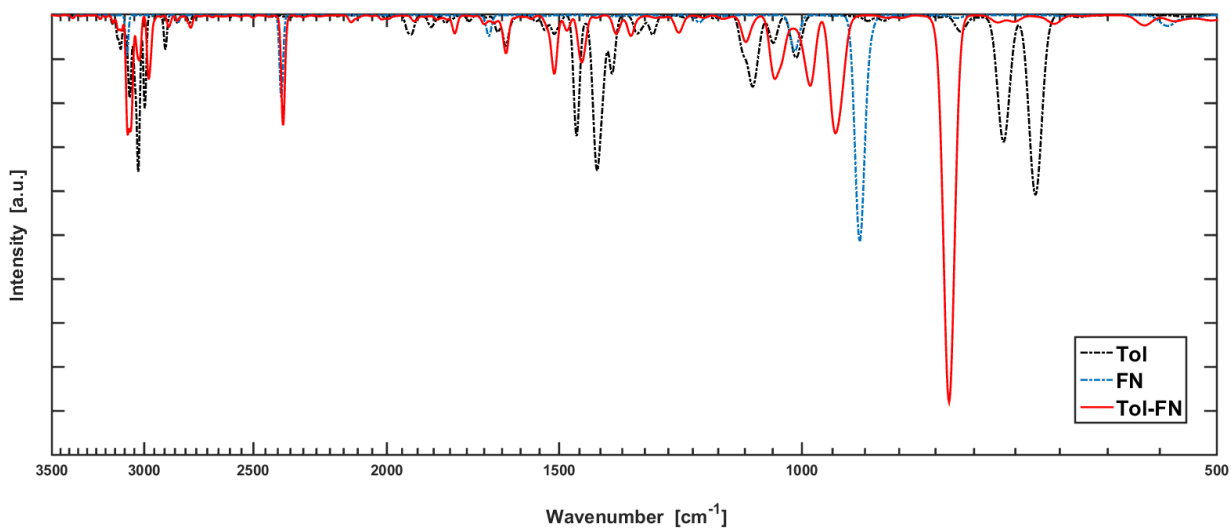
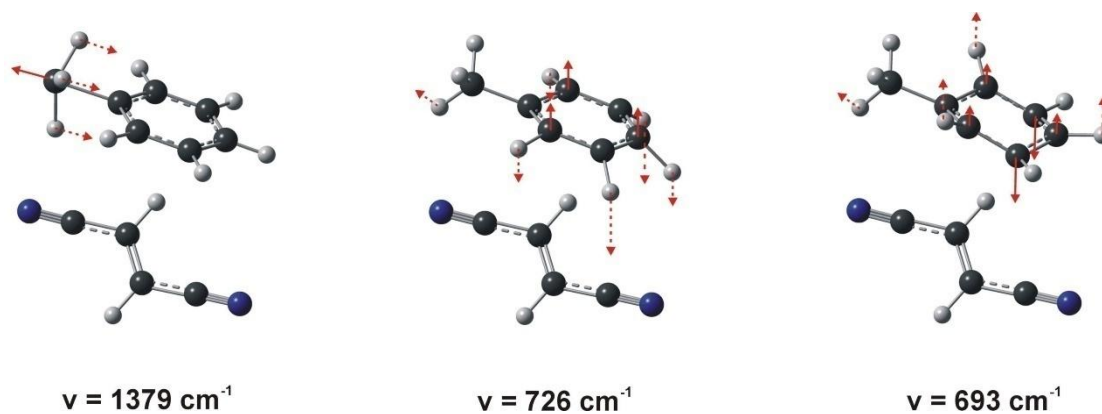


Fig. S.5b Simulated infrared spectra same as in **Fig. S.5a**, but obtained with M06-2X method.

Table S.3 Evolution of the positions of the extrema of the bands characteristic for toluene upon the contact with a crystal of fumaronitrile.

Spectrum	Band extrema positions [cm^{-1}]							
PureTol	692.66	725.74	1029.73	1080.74	1178.18	1378.66	1494.94	1604.00
FN + 2d Tol	693.48	727.38	1029.64	1081.10	1178.53	1380.56	1494.80	1603.55
FN + 1d Tol	694.07	728.69	1029.51	1081.28	1178.38	1381.30	1494.96	1603.50

1d / 2d – one / two droplets of toluene deposited on a crystal of FN; **bold** – noticeable change; the values of the band extrema positions were read upon a least square fitting of Gaussian profiles to spectral line data;



Rys. S.6 Normal modes of the toluene molecule that noticeably change their vibrational energy upon contact with the fumaronitrile molecule (see **Fig. 4** and **Tab. S.3**).

3.3 Characteristics of vertical electronic excitations

Tab. S.4 Energies [nm] of the first three electronic transitions ($S_0 \rightarrow S_1$, S_2 , S_3) occurring in the Tol-FN complex, compared to $S_0 \rightarrow S_1$ excitations calculated for the isolated molecules in vacuum.

	B3LYP		CAM-B3LYP		PBE0		MP2	
	TD	TDA	TD	TDA	TD	TDA	CIS(D)	CIS
Tol	235.6	234.4	228.8	226.5	230.5	229.1	239.7	209.5
FN	232.0	228.5	219.0	207.7	227.5	223.7	193.7	214.0
Tol-FN	369.4	369.0	272.4	272.1	342.6	342.2	227.5	218.2
	341.0	340.4	255.6	254.9	316.4	315.8	221.3	209.7
	234.9	233.5	227.7	225.4	230.0	228.4	217.8	208.5
	M06-L		M06-2X		M06-HF		LC- ω PBE	
	TD	TDA	TD	TDA	TD	TDA	TD	TDA
Tol	234.0	232.9	226.7	224.4	219.9	215.3	224.3	220.1
FN	237.8	237.7	215.5	212.3	245.3	220.8	208.1	197.6
Tol-FN	432.1	431.2	272.8	272.2	245.5	222.0	225.0	222.5
	393.5	392.6	257.0	256.0	239.7	219.6	223.8	220.5
	248.9	248.8	226.2	223.8	223.8	215.6	211.6	208.9

Tab. S.5 Energies (λ) and oscillator strengths (f) of the lowest vertical energy transitions for toluene, fumaronitrile and their complex in vacuum (M06-2X).

	TD-M06-2X				TDA-M06-2X			
	Complex		Moieties		Complex		Moieties	
	λ [nm]	f	λ [nm]	f	λ [nm]	f	λ [nm]	f
CT	272.8	0.015	-	-	272.2	0.016		
	257.0	0.015	-	-	256.0	0.013		
Tol	226.2	0.004	226.7	0.002	223.8	0.002	224.4	0.002
FN	216.3	0.277	215.5	0.521	211.3	0.007	212.3	0.000
					204.8	0.370	204.5	0.000
							203.4	0.660

For CAM-B3LYP results, see **Tab. 2**.

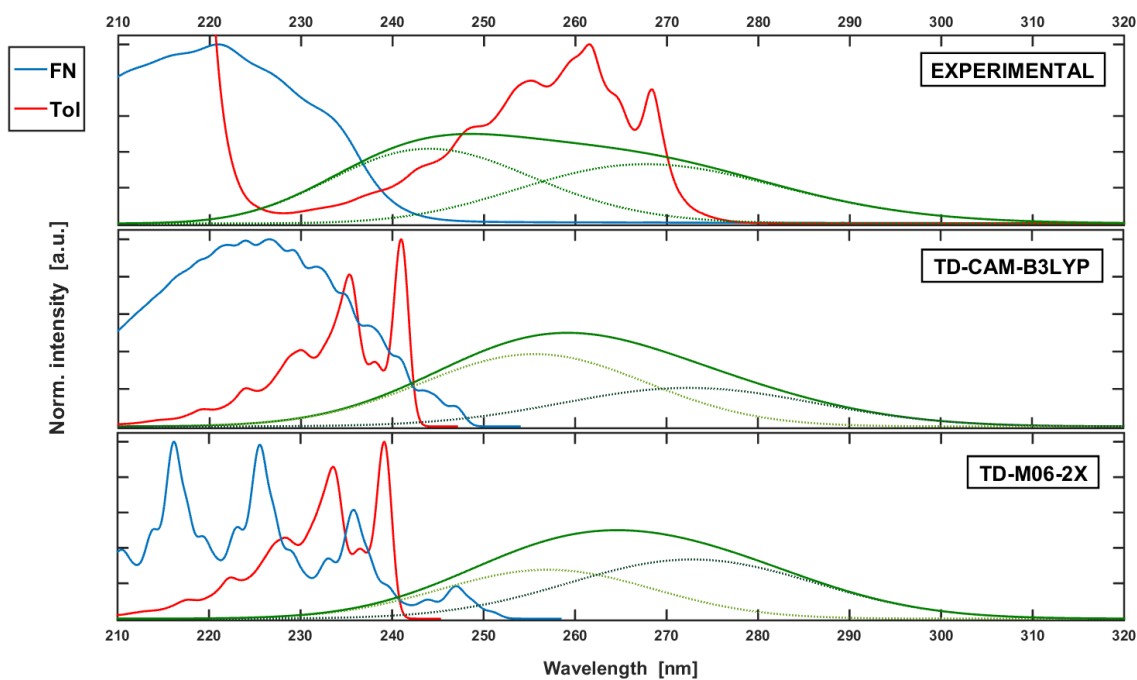


Fig. S.7 Normalized simulated and experimental (bottom, see **Fig. S.9**) UV-Vis spectra originating from excitation of toluene (red), fumaronitrile (blue) and CT transitions between them (green; broken lines – two transition components).

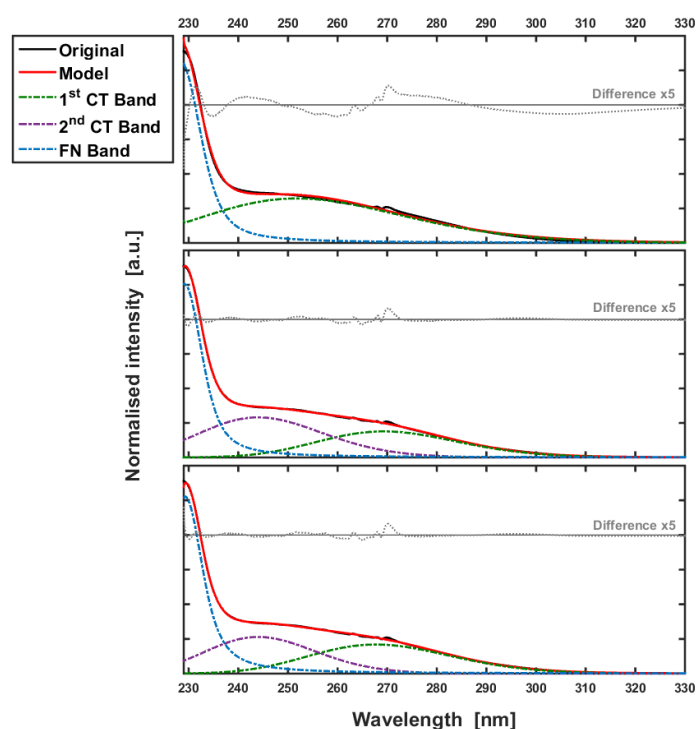


Fig. S.8 Fit of several possible combinations of bell-shaped Voigt curves, reproducing the spectrum of fumaronitrile and charge-transfer band. Differences between the modeled and measured spectra are marked with grey. Optimization has been performed in the wavenumber domain.

Tab. S.6 Energies [nm] and oscillator strengths (in parenthesis) of the photoinduced CT transitions (rows 1-2) and local toluene excitation (3rd row), calculated for the Tol-FN complex in several solvents. Simulations were performed with (equilibrium) and without (state-specific) equilibration of the solvent surrounding the adduct after its excitation.

Vapour $\epsilon = 1.00$	Equilibrium			State-specific		
	Toluene $\epsilon = 2.37$	n-Pentanol $\epsilon = 15.13$	Acetonitrile $\epsilon = 35.69$	Toluene $\epsilon = 2.37$	n-Pentanol $\epsilon = 15.13$	Acetonitrile $\epsilon = 35.69$
TDA-CAM-B3LYP						
272.11 (0.0115)	275.38 (0.0134)	275.11 (0.0135)	274.80 (0.0133)	343.05 (0.0104)	333.29 (0.0108)	324.96 (0.0108)
254.86 (0.0197)	258.26 (0.0231)	258.60 (0.0199)	258.41 (0.0190)	316.60 (0.0170)	309.25 (0.0148)	302.22 (0.0145)
225.37 (0.0025)	225.66 (0.0033)	225.56 (0.0027)	225.51 (0.0025)	225.64 (0.0017)	225.54 (0.0015)	225.49 (0.0015)
TDA-M06-2X						
272.22 (0.0163)	274.56 (0.0199)	277.78 (0.0256)	273.75 (0.0192)	332.30 (0.0156)	325.57 (0.0207)	316.73 (0.0159)
255.96 (0.0134)	258.43 (0.0172)	261.27 (0.0052)	258.45 (0.0142)	308.95 (0.0124)	303.25 (0.0052)	296.48 (0.0106)
223.84 (0.0024)	224.06 (0.0029)	223.57 (0.0040)	223.91 (0.0027)	224.21 (0.0016)	223.76 (0.0020)	224.03 (0.0016)
TDA-M06-HF						
206.69 (0.0766)	208.45 (0.1092)	208.10 (0.0810)	207.96 (0.0759)	239.82 (0.0447)	236.12 (0.0425)	232.77 (0.0416)
199.42 (0.0208)	200.93 (0.0290)	200.75 (0.0442)	200.54 (0.0424)	229.29 (0.0091)	225.93 (0.0075)	223.64 (0.0050)
222.01 (0.0016)	221.25 (0.0332)	221.11 (0.0300)	221.03 (0.0283)	214.76 (0.0029)	213.61 (0.0011)	213.10 (0.0012)

Relative dielectric constant, ϵ_{rel} , taken from [16];

3.4 Thermodynamic parameters

Tab. S.7 'Crude' values of enthalpy (ΔH), entropy (ΔS) and equilibrium constant K_x (S.6) of Tol-FN complex formation, predicted by different computational methods.

Solvent:	Vapour $\epsilon = 1.00$	Toluene $\epsilon = 2.37$	THF $\epsilon = 7.43$	n-Pentanol $\epsilon = 15.13$	Ethanol $\epsilon = 24.85$	Acetonitrile $\epsilon = 35.69$
Enthalpy ΔH [kJ/mol]						
B3LYP	-26.21	-21.71	-	-17.21	-	-16.49
CAM-B3LYP	-25.86	-21.09	-17.34	-16.25	-15.82	-15.61
M06-L	-26.75	-23.65	-20.50	-19.59	-19.24	-19.07
M06-2X	-30.97	-25.86	-22.35	-22.06	-20.82	-20.02
M06-HF	-41.56	-36.01	-31.50	-30.15	-29.56	-29.31
PBE0	-28.27	-23.49	-19.67	-18.54	-18.08	-17.86
MP2	-40.17	-35.74	-	-34.04	-	-33.54
LC- ω PBE	-30.13	-25.24	-	-21.60	-	-20.23
Entropy ΔS [J/mol·K]						
B3LYP	-126.23	-125.10	-	-124.55	-	-127.63
CAM-B3LYP	-123.68	-126.78	-127.43	-127.88	-128.52	-129.01
M06-L	-136.21	-143.63	-139.75	-143.53	-142.66	-143.50
M06-2X	-134.03	-128.34	-137.13	-135.54	-135.05	-126.40
M06-HF	-136.98	-139.24	-142.40	-143.31	-144.30	-143.59
PBE0	-127.54	-126.29	-125.64	-125.23	-125.52	-125.65
MP2	-130.12	-130.06	-	-139.84	-	-138.93
LC- ω PBE	-135.80	-136.77	-	-142.46	-	-131.27
Equilibrium constant K_x [-]						
B3LYP	1.00E-2	1.87E-3	-	3.24E-4	-	1.68E-4
CAM-B3LYP	1.18E-2	1.19E-3	2.41E-4	1.47E-4	1.15E-4	9.93E-5
M06-L	3.74E-3	4.38E-4	1.96E-4	8.64E-5	8.32E-5	7.02E-5
M06-2X	2.68E-2	6.75E-3	5.68E-4	6.13E-4	3.93E-4	8.06E-4
M06-HF	1.3461	0.109	0.012	0.0063	0.0044	0.0043
PBE0	1.97E-2	3.31E-3	7.67E-4	5.10E-4	4.09E-4	3.69E-4
MP2	1.76	0.30	-	0.05	-	0.0418
LC- ω PBE	1.54E-2	1.90E-3	-	2.21E-4	-	4.89E-4

Relative dielectric constant, ϵ_{rel} , taken from [16];

Tab. S.8 Estimated energies ΔH_{solv} [kJ/mol] of unspecific, solvent-like interaction between fumaronitrile and toluene molecules, used for (S.7) correction (see SI - Section 2.2).

B3LYP	CAM-B3LYP	M06-L	M06-2X	M06-HF	PBE0	MP2	LC- ω PBE
-14.3	-14.82	-12.94	-14.01	-14.32	-14.03	-12.95	-14.70

Tab. S.9 Corrected values of enthalpy (ΔH) (S.7), entropy (ΔS) (S.8b) and equilibrium constant K_C (S.8a) of Tol-FN complex formation, predicted by different computational methods (see Tab. S.7).

Solvent:	Vapour $\epsilon = 1.00$	Toluene $\epsilon = 2.37$	THF $\epsilon = 7.43$	n-Pentanol $\epsilon = 15.13$	Ethanol $\epsilon = 24.85$	Acetonitrile $\epsilon = 35.69$
Enthalpy ΔH [kJ/mol]						
B3LYP	-14.30	-11.91	-7.41	-	-2.91	-
CAM-B3LYP	-14.82	-11.05	-6.27	-2.52	-1.43	-1.00
M06-L	-12.94	-12.94	-9.83	-6.68	-5.78	-5.42
M06-2X	-14.01	-16.96	-11.85	-8.34	-8.06	-6.81
M06-HF	-14.32	-27.23	-21.69	-17.18	-15.83	-15.24
PBE0	-14.03	-14.24	-9.46	-5.64	-4.51	-4.05
MP2	-12.95	-27.22	-	-22.79	-	-21.09
LC- ω PBE	-15.43	-10.54	-	-6.90	-	-5.53
Entropy ΔS [J/mol·K]						
B3LYP	-51.67	-50.54	-	-49.99	-	-53.07
CAM-B3LYP	-47.38	-50.48	-51.13	-51.58	-52.22	-52.71
M06-L	-63.28	-70.70	-66.82	-70.60	-69.73	-70.57
M06-2X	-60.44	-54.74	-63.53	-61.95	-61.46	-52.81
M06-HF	-62.34	-64.60	-67.76	-68.67	-69.66	-68.95
PBE0	-56.00	-54.75	-54.10	-53.69	-53.98	-54.10
MP2	-60.08	-60.02	-	-69.80	-	-68.89
LC- ω PBE	-59.89	-60.86	-	-66.55	-	-55.36
Equilibrium constant K_C [-]						
B3LYP	0.2453	0.0457		0.0079		0.0041
CAM-B3LYP	0.2891	0.0290	0.0059	0.0036	0.0028	0.0024
M06-L	0.0916	0.0107	0.0048	0.0021	0.0020	0.0017
M06-2X	0.6549	0.1651	0.0139	0.0150	0.0096	0.0197
M06-HF	32.9229	2.6731	0.2965	0.1541	0.1077	0.1059
PBE0	0.4812	0.0811	0.0188	0.0125	0.0100	0.0090
MP2	42.9926	7.2376	-	1.1248	-	1.02
LC- ω PBE	0.3767	0.0465	-	0.0054	-	0.0120

Relative dielectric constant, $\epsilon_{rel.}$, taken from [16];

3.5 Fluorescence in the system

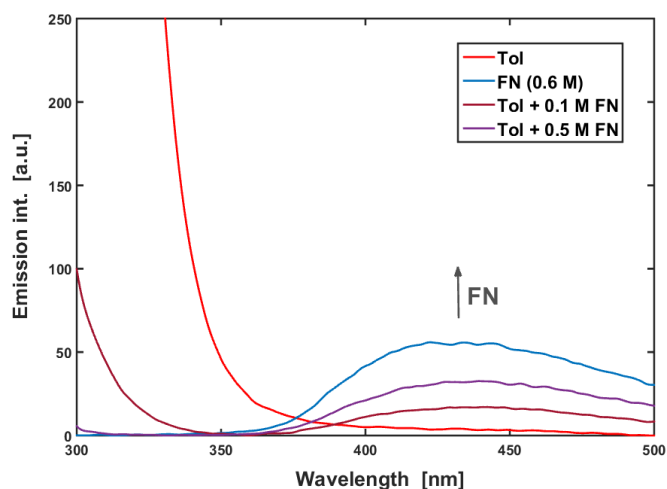


Fig. S.9 Fluorescence spectra of toluene, fumaronitrile and their mixture, recorded in ethyl acetate. No 'new' band, resulting from toluene-fumaronitrile interaction is present in the system. The wide band, with maxima at c.a. 440 nm, originates from the fumaronitrile sample, since it is also observed for the concentrated solution of 'pure' FN. Most probably it is due to traces of carbonyl type derivatives [17] of fumaronitrile that are reported to be the main post-synthetic contamination of the commercially obtained samples [18].

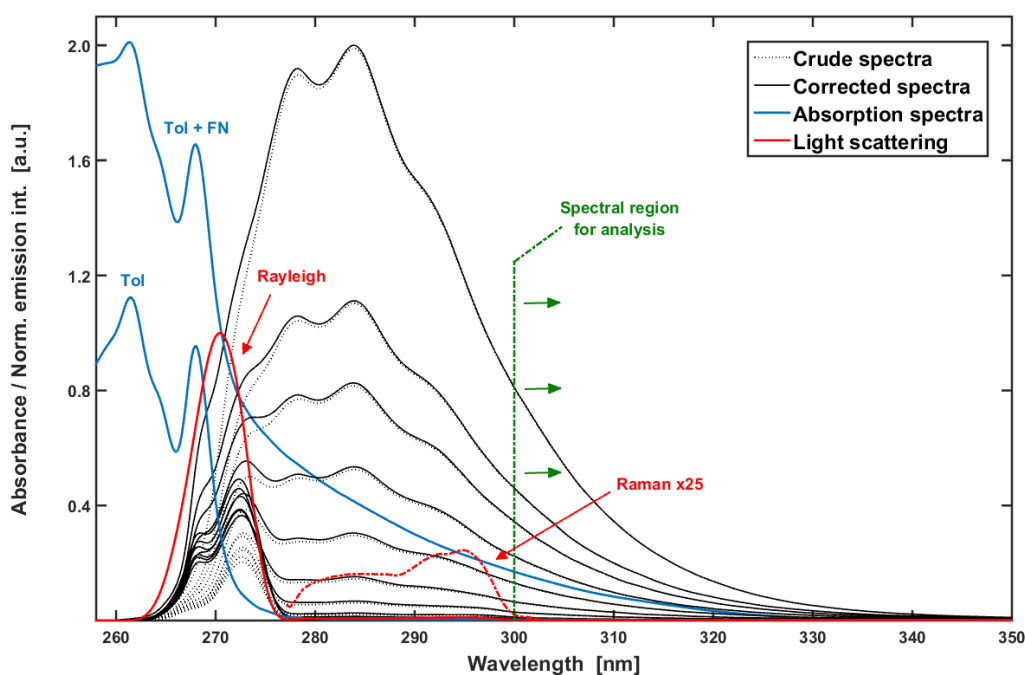


Fig. S.10 Normalized spectra of fluorescence of toluene quenched by fumaronitrile before (dotted lines) and after (solid lines) the self-absorption correction (S.9). Two limiting absorption spectra of the samples, used among other for this correction, are presented in blue. Light scattering observed in the system is illustrated with a signal recorded for the pure solvent (ethyl acetate) and shown in red. Green vertical line refer to the spectral region free from the scattered light.

4. References

- [1] W.E. Wentworth, W. Hirsch, E. Chen, Rigorous least-squares estimation of molecular complex equilibria. I. Single intermolecular complex utilizing spectrophotometric data, *The Journal of Physical Chemistry*, 1967, **71**: 218-231
- [2] K. Hirose, A practical guide for the determination of binding constants, *Journal of Inclusion Phenomena and Macrocyclic Chemistry*, 2001, **39**: 193-209
- [3] P. Thordarson, Determining association constants from titration experiments in supramolecular chemistry, *Chemical Society Reviews*, 2011, **40**: 1305-1323
- [4] H.A. Benesi, J.H. Hildebrand, A spectrophotometric investigation of the interaction of iodine with aromatic hydrocarbons, *Journal of the American Chemical Society*, 1949, **71**: 2703-2707
- [5] N.J. Rose, R.S. Drago, Molecular addition compounds of iodine. I. An absolute method for the spectroscopic determination of equilibrium constants. *Journal of the American Chemical Society*, 1959, **81**: 6138-6141
- [6] OriginPro 9.1, OriginLab Corporation, Northampton, 2014
- [7] E.C.W Clarke, D.N. Glew, Evaluation of thermodynamic functions from equilibrium constants, *Transactions of the Faraday Society*, 1966, **62**: 539-547
- [8] S.F. Dec, S.J. Gill, Temperature dependence of errors in parameters derived from van't Hoff studies, *Journal of Chemical Education*, 1985, **62**: 879
- [9] T. Galaon, V. David, Deviation from van't Hoff dependence in RP-LC induced by tautomeric interconversion observed for four compounds. *Journal of Separation Science*, 2011, **34**: 1423-1428.
- [10] B.B. Benson, D. Krause, Empirical laws for dilute aqueous solutions of nonpolar gases, *The Journal of Chemical Physics*, 1976, **64**: 689-709
- [11] M. Maeder, Y.M. Neuhold, Practical Data Analysis in Chemistry, Elsevier, Amsterdam, 2007
- [12] A.J. Kalka, A.M. Turek, Compensation of temperature effects on spectra through evolutionary rank analysis, *Spectrochimica Acta Part A: Molecular and Biomolecular Spectroscopy*, 2020, **245**: 118770
- [13] P.H.C. Eilers A perfect smoother, *Analytical Chemistry*, 2003, **75**: 631-636
- [14] J.F. Holland, R.E. Teets, P.M. Kelly, A. Timnick, Correction of right-angle fluorescence measurements for the absorption of excitation radiation, *Analytical chemistry*, 1977, **49**: 706-710
- [15] J.R. Lakowicz, Principles of Fluorescence Spectroscopy, Springer, Boston MA, 2006
- [16] M.J. Frisch, G.W. Trucks, H.B. Schlegel, G.E. Scuseria, M.A. Robb, J.R. Cheeseman, G. Scalmani, V. Barone, G. A. Petersson, H. Nakatsuji, X. Li, M. Caricato, A.V. Marenich, J. Bloino, B.G. Janesko, R. Gomperts, B. Mennucci, H. P. Hratchian, J.V. Ortiz, A.F. Izmaylov, J.L. Sonnenberg, D. Williams-Young, F. Ding, F. Lipparini, F. Egidi, J. Goings, B. Peng, A. Petrone, T. Henderson, D. Ranasinghe, V.G. Zakrzewski, J. Gao, N. Rega, G. Zheng, W. Liang, M. Hada, M. Ehara, K. Toyota, R. Fukuda, J. Hasegawa, M. Ishida, T. Nakajima, Y. Honda, O. Kitao, H. Nakai, T. Vreven, K. Throssell, J.A. Montgomery, J.E. Peralta, F. Ogliaro, M.J. Bearpark, J.J. Heyd, E.N. Brothers, K.N. Kudin, V.N. Staroverov, T.A. Keith, R. Kobayashi, J. Normand, K. Raghavachari, A.P. Rendell, J.C. Burant, S.S. Iyengar, J. Tomasi, M. Cossi, J.M. Millam, M. Klene, C. Adamo, R. Cammi, J.W. Ochterski, R.L. Martin, K. Morokuma, O. Farkas, J.B. Foresman, D.J. Fox, Gaussian 16 (Revision A.03), Gaussian Inc., Wallingford CT, 2016
- [17] S. Lind, J. Trost, L. Zigan, A. Leipertz, S. Will, S. Application of the tracer combination TEA/acetone for multi-parameter laser-induced fluorescence measurements in IC engines with exhaust gas recirculation, *Proceedings of the Combustion Institute*, 2015, **35**: 3783-3791
- [18] D.T. Mowry, J.M. Butler, Fumaronitrile, *Organic Syntheses*, 2003, **30**: 46-46